Stabilization of the Resistive Wall Mode Using a Fake Rotating Shell

Richard Fitzpatrick and Torkil H. Jensen[a)]
Institute for Fusion Studies
The University of Texas at Austin
Austin, Texas 78712 USA

Abstract

Tokamak plasma performance can, in theory, be greatly improved if the so called "resistive wall mode" is stabilized. This can be achieved by spinning the plasma rapidly, but such a scheme is not reactor relevant. A more promising approach is to apply external feedback in order to make a resistive shell placed around the plasma act like a perfect conductor. A scheme is outlined by which a network of feedback controlled conductors surrounding the plasma can be made to act like a *rotating* shell. This fake rotating shell combined with a stationary conventional shell (e.g. the vacuum vessel) can completely stabilize the resistive wall mode. The gain, bandwidth, current, and power requirements of the feedback amplifiers are extremely modest. A previously proposed stabilization scheme (the intelligent shell) is also investigated, and is compared with the fake rotating shell concept. The main disadvantage of the former scheme is that it requires a high gain.

[a)]General Atomics, La Jolla, CA

1 Introduction

Present day tokamak performance is often limited by pressure driven external kink modes [1]. The ideal external kink mode can be completely stabilized by placing a perfectly conducting shell sufficiently close to the plasma [2]. However, the best that a resistive shell can do is to convert the fast growing ideal mode into the much slower growing resistive shell (or resistive wall) mode [3]. The resistive shell mode is dangerous because tokamak discharges typically last much longer than its e-folding time.

There are two possible approaches to stabilizing the resistive shell mode. The first is to modify the plasma somehow; e.g. by making it rotate rapidly [4]. Unfortunately, it is difficult to envisage a reactor possessing sufficient plasma rotation to achieve stabilization, because of the large volume of the plasma plus the fact that neutral beam injection (the most commonly used scheme for spinning plasmas) must be performed with high energy (i.e. low momentum) particles in a large device. The second, more reactor relevant, approach is to modify the shell; e.g. by making it act like a perfect conductor [5]. This paper will investigate the second approach.

2 The Fake Shell

2.1 Introduction

Consider a large aspect ratio, low β, tokamak plasma whose magnetic flux surfaces map out (almost) concentric circles in the poloidal plane. Such a tokamak is well approximated as a periodic cylinder. Standard cylindrical polar coordinates (r, θ, z) are adopted. The system is assumed to be periodic in the z direction, with periodicity length $2\pi R_0$, where R_0 is the simulated major radius of the device. It is convenient to define a simulated toroidal angle $\phi = z/R_0$.

2.2 Preliminary Analysis

Consider a fake shell, surrounding the plasma, which is made up of a uniform two dimensional network of resistors and inductors (see Fig. 1). Let $\Delta\theta$ and $\Delta\phi$ be the angular spacings of the network in the poloidal and toroidal directions, respectively.

Suppose that a current $J_w(\theta,\phi)$ flows around the network loop centred on $(\theta,\ \phi)$. The currents flowing in the network are approximated as a smoothed out distribution with radially integrated current density $\delta\mathbf{I}_w(\theta,\phi)$. Now

$$\delta I_{w\,\theta}(\theta,\phi) \simeq \frac{J_w(\theta,\phi+\Delta\phi) - J_w(\theta,\phi)}{R_0\Delta\phi}, \tag{1)(a}$$

$$\delta I_{w\,\phi}(\theta,\phi) \simeq \frac{-J_w(\theta+\Delta\theta,\phi) + J_w(\theta,\phi)}{r_w\Delta\theta}, \tag{1)(b}$$

where r_w is the minor radius of the network. It is assumed that $r_w > a$, where a is the minor radius of the plasma. Approximating $J_w(\theta,\phi)$ as a continuous function gives

$$\delta\mathbf{I}_w \simeq \left(0, \frac{1}{R_0}\frac{\partial J_w}{\partial\phi}, -\frac{1}{r_w}\frac{\partial J_w}{\partial\theta}\right), \tag{2}$$

so that

$$\delta\mathbf{I}_w \simeq \nabla\wedge(J_w\,\hat{\mathbf{r}}) \equiv \nabla J_w\wedge\hat{\mathbf{r}}. \tag{3}$$

Thus, $J_w(\theta,\phi)$ is the stream function for the effective continuous current distribution flowing in the fake shell.

The circuit equation for the loop centred on $(\theta,\ \phi)$ is

$$\begin{aligned} -\gamma\,\delta B_{r\,\text{plasma}}\,\Delta A &- \gamma L_\phi(\,J_w(\theta,\phi) - J_w(\theta+\Delta\theta,\phi)\,) \\ &- \gamma L_\phi(\,J_w(\theta,\phi) - J_w(\theta-\Delta\theta,\phi)\,) \\ &- \gamma L_\theta(\,J_w(\theta,\phi) - J_w(\theta,\phi+\Delta\phi)\,) \\ &- \gamma L_\theta(\,J_w(\theta,\phi) - J_w(\theta,\phi-\Delta\phi)\,) \end{aligned}$$

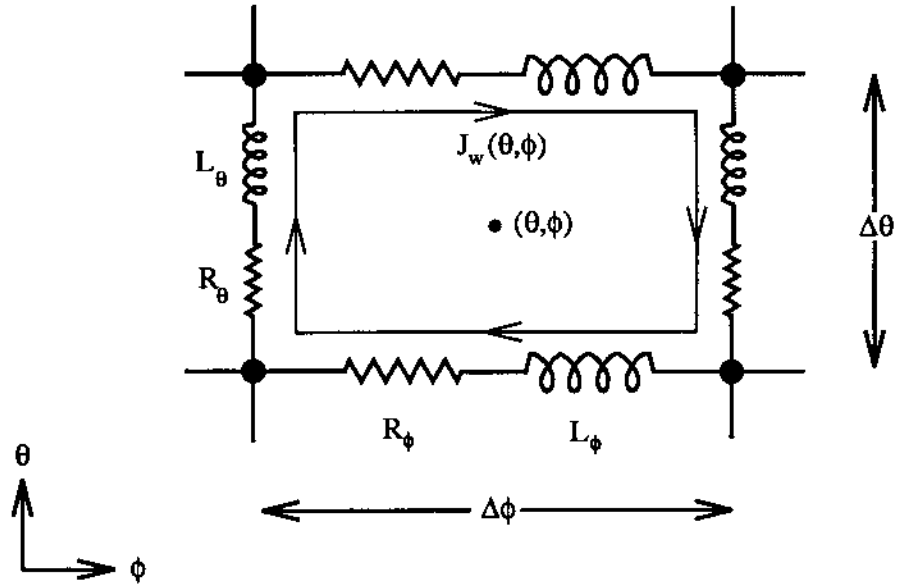

Figure 1: *Schematic diagram showing a single loop of a uniform two dimensional network of resistors and inductors surrounding the plasma. The loop is centred on the point* (θ, ϕ). *The resistances of the poloidal and toroidal legs of the loop are* R_θ *and* R_ϕ, *respectively. The inductances of the poloidal and toroidal legs are* L_θ *and* L_ϕ, *respectively. The current which flows around the loop is denoted* $J_w(\theta, \phi)$.

$$= \tag{4}$$

$$+ R_\phi(J_w(\theta,\phi) - J_w(\theta + \Delta\theta, \phi))$$

$$+ R_\phi(J_w(\theta,\phi) - J_w(\theta - \Delta\theta, \phi))$$

$$+ R_\theta(J_w(\theta,\phi) - J_w(\theta, \phi + \Delta\phi))$$

$$+ R_\theta(J_w(\theta,\phi) - J_w(\theta, \phi - \Delta\phi)).$$

Here, γ is the growth rate, $\delta B_{r\,\mathrm{plasma}}(\theta, \phi)$ is the (approximately uniform) radial magnetic field at the loop due to plasma currents, and $\Delta A = r_w R_0 \Delta\theta\Delta\phi$ is the area of the loop. It is assumed that $\delta B_{r\,\mathrm{plasma}}(\theta, \phi)$ varies poloidally and toroidally on angular scales which are much longer than $\Delta\theta$ and $\Delta\phi$, respectively.

Let

$$\delta\mathbf{B} = \nabla \wedge (\psi\,\hat{\mathbf{z}}) \equiv \nabla\psi \wedge \hat{\mathbf{z}}, \tag{5}$$

where $\psi(r,\theta,\phi)$ is the perturbed poloidal magnetic flux, and $\Psi_w(\theta,\phi) \equiv \psi(r_w,\theta,\phi)$ is the flux in the shell. Consider the m/n external kink mode, for which

$$\psi(r,\theta,\phi) = \widehat{\psi}(r)\exp[\,\mathrm{i}\,(m\theta - n\phi)], \tag{6}(a)$$

$$\Psi_w(\theta,\phi) = \widehat{\Psi}_w\exp[\,\mathrm{i}\,(m\theta - n\phi)], \tag{6}(b)$$

$$J_w(\theta,\phi) = \widehat{J}_w\exp[\,\mathrm{i}\,(m\theta - n\phi)], \tag{6}(c)$$

where $\widehat{\Psi}_w \equiv \widehat{\psi}(r_w)$. The network currents can only be approximated as a smoothed out current distribution provided that

$$m\,\Delta\theta \ll 2\pi, \tag{7}(a)$$

$$n\,\Delta\phi \ll 2\pi; \tag{7}(b)$$

i.e. there is very little phase variation of the mode from loop to loop.

The shell stability index for the m/n mode is defined

$$\Delta_w = \left[r\frac{d\widehat{\psi}}{dr}\Big/\,\widehat{\psi}\right]_{r_{w-}}^{r_{w+}}. \tag{8}$$

Ampére's law integrated across the network yields

$$\mathrm{i}\,m\mu_0\widehat{J}_w = \Delta_w\,\widehat{\Psi}_w. \tag{9}$$

The perturbed poloidal flux function $\widehat{\psi}(r)$ can be written in the form

$$\widehat{\psi}(r) = \left(1 + \frac{\Delta_w}{2m}\right)\widehat{\Psi}_w\widehat{\psi}_{\mathrm{plasma}}(r) - \frac{\Delta_w}{2m}\widehat{\Psi}_w\widehat{\psi}_{\mathrm{shell}}(r) \tag{10}$$

outside the plasma, where $\widehat{\psi}_{\mathrm{plasma}}(r)$ is that part of the flux function which is maintained by plasma currents and $\widehat{\psi}_{\mathrm{shell}}(r)$ is that part which is maintained by currents flowing in the

fake shell. Both $\widehat{\psi}_{\rm plasma}$ and $\widehat{\psi}_{\rm shell}$ are normalized to unity at the network radius. Note that $\widehat{\psi}_{\rm plasma}$ is continuous across the network whereas $\widehat{\psi}_{\rm shell}$ has a gradient discontinuity. It is easily demonstrated that

$$\widehat{\psi}_{\rm shell}(r) = \left(\frac{r}{r_w}\right)^{+m} \quad \text{for } r < r_w, \tag{11}(a)$$

$$\widehat{\psi}_{\rm shell}(r) = \left(\frac{r}{r_w}\right)^{-m} \quad \text{for } r \geq r_w. \tag{11}(b)$$

It follows from Eqs. (5), (6)(a), and (10) that

$$\delta B_{r\,\rm plasma} = \mathrm{i}\,\frac{m}{r}\left(1+\frac{\Delta_w}{2m}\right)\widehat{\Psi}_w. \tag{12}$$

Equations (4), (6), and (12) yield

$$\mathrm{i}\,\gamma m R_0 \Delta\theta\Delta\phi\left(1+\frac{\Delta_w}{2m}\right)\widehat{\Psi}_w \simeq -(R_\phi+\gamma L_\phi)(m\Delta\theta)^2\widehat{J}_w$$

$$-(R_\theta+\gamma L_\theta)(n\Delta\phi)^2\widehat{J}_w. \tag{13}$$

Equations (9) and (13) combine to give

$$\Delta_w = \frac{\gamma\mu_0 m^2 R_0\Delta\theta\Delta\phi(1+\Delta_w/2m)}{(R_\phi+\gamma L_\phi)(m\Delta\theta)^2+(R_\theta+\gamma L_\theta)(n\Delta\phi)^2}, \tag{14}$$

which can also be written

$$\gamma\tau_w = \frac{\Delta_w}{1-\Delta_w/\Delta_c}, \tag{15}$$

where

$$\tau_w = \frac{\mu_0 m^2 R_0\Delta\theta\Delta\phi}{R_\phi(m\Delta\theta)^2+R_\theta(n\Delta\phi)^2}, \tag{16}$$

and

$$\Delta_c = \frac{\mu_0 m^2 R_0\Delta\theta\Delta\phi}{\tilde{L}_\phi(m\Delta\theta)^2+L_\theta(n\Delta\phi)^2}. \tag{17}$$

Here,

$$\tilde{L}_\phi = L_\phi - \frac{\mu_0 R_0}{2m}\frac{\Delta\phi}{\Delta\theta}. \tag{18}$$

Equation (15) can be written in the form

$$\gamma\hat{\tau}_w = \hat{\Delta}_w, \tag{19}$$

where $\hat{\Delta}_w$ is the stability index for a shell located at radius

$$\hat{r}_w = r_w\left(1+\frac{2m}{\Delta_c}\right)^{1/2m}, \tag{20}$$

and

$$\hat{\tau}_w = \tau_w\left(1+\frac{2m}{\Delta_c}\right). \tag{21}$$

Equation (19) is obtained from Eq. (15) by noting that $\nabla^2\psi = 0$ in the vacuum region outside the plasma, so $\widetilde{\psi}(r)$ is a linear combination of r^{+m} and r^{-m} solutions in this region. Recall that the dispersion relation for a conventional resistive shell is $\gamma\tau_w = \Delta_w$ [6], where Δ_w is the shell stability index (see Eq. (8)), and τ_w is the time constant (or L/R time) of the shell. It is clear that the network acts like a complete resistive shell whose radius $\hat{r}_w$ is somewhat larger than r_w (the actual radius of the network). The ideal stability limit corresponds to $\Delta_w \geq \Delta_c$ (or $\hat{\Delta}_w \rightarrow +\infty$). Note that the ideal mode escapes through the holes in the network, so it is not shielded from the region $r > r_w$, as would be the case for a complete shell. In fact, the network acts very much like an *incomplete* shell. (Equation (15) has the same form as the dispersion relation for an incomplete resistive shell located at radius r_w [6].)

2.3 The Fake Rotating Shell

Consider, for the sake of simplicity, the limit in which the poloidal inductance and resistance of the network are negligible. This limit corresponds to $n^2 r_w \Delta\phi \ll m^2 R_0 \Delta\theta$ if the inductance and resistance per unit length are the same in the poloidal and toroidal directions. Suppose that each loop in the network is accompanied by a high impedance sensor loop of equal area which measures the local rate of change of the magnetic flux escaping through the network (see Fig. 2).

The voltage generated in the sensor loop centred on (θ, ϕ) is $\widehat{V}(t)\exp[\mathrm{i}\,(m\theta - n\phi)]$, where

$$\widehat{V}(t) \simeq -\frac{d}{dt}\left(\mathrm{i}\,mR_0\Delta\theta\Delta\phi\left(1+\frac{\Delta_w}{2m}\right)\widehat{\Psi}_w(t) + L_\phi(m\Delta\theta)^2\widehat{J}_w(t)\right). \tag{22}$$

This signal can be integrated to give

$$\begin{aligned}\widehat{\mathcal{V}}(t) &= \int_0^t \widehat{V}(t)\,dt \\ &\simeq -\left(\mathrm{i}\,mR_0\Delta\theta\Delta\phi\left(1+\frac{\Delta_w}{2m}\right)\widehat{\Psi}_w(t) + L_\phi(m\Delta\theta)^2\widehat{J}_w(t)\right),\end{aligned} \tag{23}$$

assuming that the mode amplitude is negligibly small at time $t = 0$. Suppose that the integrated signal is amplified by a factor $1/\tau$ and then fed back into the network (see Fig. 2). The modified circuit equation for the network loop centred on (θ, ϕ) is

$$\begin{aligned}&\left(\widehat{V}(t) + \frac{\widehat{\mathcal{V}}(t)}{\tau} - \frac{\widehat{\mathcal{V}}(t)\exp(\mathrm{i}\,m\Delta\theta)}{\tau}\right)\exp[\mathrm{i}\,(m\theta - n\phi)] \\ &\qquad \simeq R_\phi(m\Delta\theta)^2\widehat{J}_w(t)\exp[\mathrm{i}\,(m\theta - n\phi)],\end{aligned} \tag{24}$$

giving

$$\widehat{V}(t) - \mathrm{i}\,\frac{m\Delta\theta}{\tau}\widehat{\mathcal{V}}(t) \simeq R_\phi(m\Delta\theta)^2\widehat{J}_w(t). \tag{25}$$

Equations (22) and (25) yield

$$\mathrm{i}\,\tilde{\gamma}mR_0\Delta\theta\Delta\phi\left(1+\frac{\Delta_w}{2m}\right)\widehat{\Psi}_w \simeq -(R_\phi + \tilde{\gamma}L_\phi)(m\Delta\theta)^2\widehat{J}_w, \tag{26}$$

where

$$\tilde{\gamma} = \gamma - \mathrm{i}\,\frac{m\Delta\theta}{\tau}. \tag{27}$$

Equations (9) and (26) combine to give

$$\gamma \simeq -\mathrm{i}\,\frac{m}{r_w}v_\theta + \frac{\Delta_w/\tau_w}{1-\Delta_w/\Delta_c}, \tag{28}$$

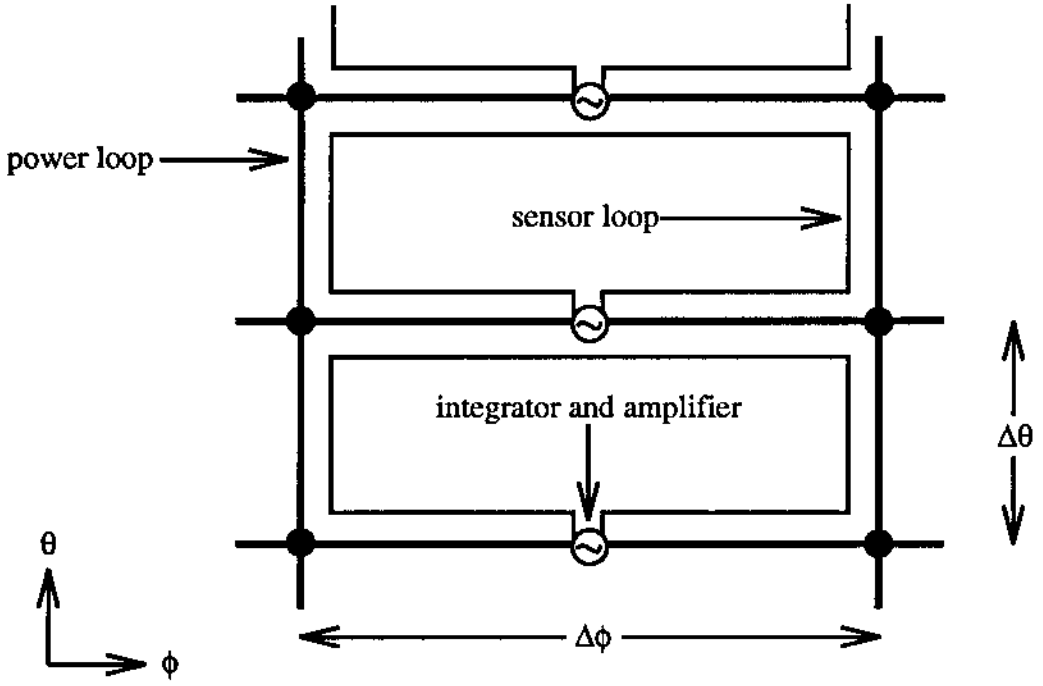

Figure 2: *Schematic diagram showing a few loops of a uniform two dimensional network of resistors and inductors, surrounding the plasma, which is subject to feedback. The low impedance loops containing the resistors and inductors are denoted the power loops (the resistors and inductors are not shown for the sake of clarity). The signals detected by the high impedance sensor loops are integrated, amplified, and then fed into the power loops, as shown.*

where

$$\tau_w \simeq \frac{\mu_0 m^2 R_0 \Delta\theta \Delta\phi}{R_\phi (m\Delta\theta)^2}, \tag{29}(a)$$

$$\Delta_c \simeq \frac{\mu_0 m^2 R_0 \Delta\theta \Delta\phi}{\tilde{L}_\phi (m\Delta\theta)^2}, \tag{29}(b)$$

and

$$v_\theta = -\frac{r_w \Delta\theta}{\tau}. \tag{30}$$

Equation (28) can be rewritten in the form

$$\gamma \simeq -\mathrm{i}\,\frac{m}{\hat{r}_w}\,\hat{v}_\theta + \frac{\hat{\Delta}_w}{\hat{\tau}_w}, \tag{31}$$

where $\hat{v}_\theta = v_\theta\,\hat{r}_w/r_w$, $\hat{\Delta}_w$ is the stability index calculated for a shell located at radius $\hat{r}_w$

(see Eq. (20)), and $\hat{\tau}_w$ is given by Eq. (21). Equation (31) is the dispersion relation for a resistive shell located at radius $\hat{r}_w$, with time constant $\hat{\tau}_w$, *which is rotating poloidally with velocity* $\hat{v}_\theta$. Thus, the feedback causes the network to act like a rotating shell. Note that the effective rotation velocity is determined by the amplification factor $1/\tau$.

The dispersion relation for the fake rotating shell is conveniently written

$$\Delta(\gamma) = \Delta_w, \tag{32}$$

where

$$\Delta(\gamma) = \frac{\tilde{\gamma}\tau_w}{1 + \tilde{\gamma}\tau_w/\Delta_c}. \tag{33}$$

The corresponding dispersion relation for a conventional shell of time constant τ_w is $\Delta(\gamma) = \Delta_w$, where $\Delta(\gamma) = \gamma\tau_w$.

2.4 Stabilization of the Resistive Shell Mode

It is possible to stabilize the resistive shell mode using just the fake rotating shell described above, but the effective angular rotation frequency needs to be comparable to the growth rate of the free boundary ideal external kink mode (i.e. prohibitively large) [7]. A more promising approach is to combine the fake rotating shell with a conventional non-rotating shell [8].

Consider a plasma surrounded by a complete non-rotating shell (shell 1) and a network (i.e. a fake rotating shell) (shell 2). The external kink dispersion relation takes the form

$$(\Delta_1 - E_1)(\Delta_2 - E_2) - (E_{12})^2 = 0, \tag{34}$$

where

$$\Delta_1 = \gamma\tau_1, \tag{35}(a)$$

$$\Delta_2 = \frac{\tilde{\gamma}\tau_2}{1 + \tilde{\gamma}\tau_2/E_{2c}}. \tag{35}(b)$$

This dispersion relation is, in fact, analogous to that for two coupled tearing modes [9]. Here, τ_1 is the time constant (or L/R time) for the conventional shell, τ_2 is the effective time constant of the fake shell (i.e. the equivalent to τ_w in the previous analysis), and E_{2c} is the critical stability index for the fake shell (i.e. the equivalent to Δ_c in the previous analysis). E_1 is the shell stability index for shell 1, calculated assuming zero magnetic flux in shell 2. Likewise, E_2 is the shell stability index for shell 2, calculated assuming that there is zero flux in shell 1. Also,

$$E_{1\infty} = E_1 - \frac{(E_{12})^2}{E_2}, \tag{36}(a)$$

$$E_{2\infty} = E_2 - \frac{(E_{12})^2}{E_1}, \tag{36}(b)$$

are the shell stability indices for shells 1 and 2, respectively, calculated in the absence of the other shell.

In the vacuum region outside the plasma $\widehat{\psi}(r)$ is just a linear combination of r^{+m} and r^{-m} solutions. It is easily demonstrated that

$$E_2 = -\frac{2m}{1-(r_1/r_2)^{2m}} \quad \text{for } r_1 < r_2, \tag{37}(a)$$

$$E_2 = -\frac{2m}{1-(r_2/r_1)^{2m}}$$

$$\frac{(r_2/r_1)^{2m}}{1+(1-(r_2/r_1)^{2m})E_{1\infty}/2m} \quad \text{for } r_1 \geq r_2, \tag{37}(b)$$

and

$$E_{12} = \frac{2m\,(r_1/r_2)^m}{1-(r_1/r_2)^{2m}} \quad \text{for } r_1 < r_2, \tag{38}(a)$$

$$E_{12} = \frac{2m\,(r_2/r_1)^m}{1-(r_2/r_1)^{2m}} \quad \text{for } r_1 \geq r_2, \tag{38}(b)$$

with

$$E_{2\infty} = \frac{E_{1\infty}}{E_{1\infty}/E_2 + (E_{12}/E_2)^2}. \tag{39}$$

Equations (34) and (35) yield

$$\gamma^2\tau_1\tau_2(1-E_2/E_{2c})-\gamma\left[\tau_1E_2+\tau_2E_1(1-E_{2\infty}/E_{2c})-\mathrm{i}\,\Omega_2\tau_1\tau_2(1-E_2/E_{2c})\right]$$

$$+\left[E_2E_{1\infty}-\mathrm{i}\,\Omega_2\tau_2E_1(1-E_{2\infty}/E_{2c})\right]=0, \qquad (40)$$

where $\Omega_2=-m\Delta\theta/\tau$ is the effective angular rotation frequency of the fake shell.

Suppose that the time constant of the conventional shell is much greater than that of the fake shell (i.e. $\tau_1\gg\tau_2$). This is a realistic ordering since the time constant of a network (which, by definition, is mostly thin air) is likely to be comparatively short. Suppose, further, that the effective rotation frequency of the fake shell is of order its inverse time constant (i.e. $|\Omega_2|\tau_2\sim O(1)$). The two roots of Eq. (40) are

$$\gamma\tau_1\simeq\frac{E_{1\infty}\left\{1+(\Omega_2\tau_2)^2(1/E_{2\infty}-1/E_{2c})(1/E_2-1/E_{2c})\right\}}{1+(\Omega_2\tau_2)^2(1/E_2-1/E_{2c})^2}$$

$$-\frac{\mathrm{i}\,\Omega_2\tau_2(E_{12}/E_2)^2}{1+(\Omega_2\tau_2)^2(1/E_2-1/E_{2c})^2}, \qquad (41)(a)$$

$$\gamma\tau_2\simeq\frac{E_2}{1-E_2/E_{2c}}-\mathrm{i}\,\Omega_2\tau_2. \qquad (41)(b)$$

The first root corresponds to a feebly rotating mode which penetrates the stationary shell and may, or may not, penetrate the fake rotating shell, depending on its rotation velocity. The second root corresponds to a mode which penetrates and co-rotates with the fake shell but does not penetrate the stationary shell.

Suppose that the m/n free boundary external kink mode is only unstable if it can pass freely through both the real and the fake shell. This implies that $E_{1\infty}>0$ and $E_1<0$. It follows from Eqs. (37) that $E_2<0$. Thus, the second root of Eq. (40) (i.e. the one which co-rotates with the fake shell) is unconditionally stable. The first root (i.e. the feebly rotating one) is stabilized given a sufficiently large rotation rate of the fake shell. This root can be identified as the "resistive shell mode." According to Eq. (41)(a), the resistive shell mode is

stable provided

$$\Omega_2 > \Omega_{2c} = \frac{1}{\tau_2\sqrt{(1/E_{2\infty} - 1/E_{2c})(1/E_{2c} - 1/E_2)}}, \tag{42}$$

Note that stabilization is only possible if the fake shell is located sufficiently close to the plasma to convert the ideal external kink mode into a resistive shell mode in the absence of the stationary shell; i.e. if $E_{2\infty} < E_{2c}$. The stabilization criterion for the combination of a stationary shell and a fake rotating shell is basically that the rotation frequency of the fake shell should be larger than its inverse time constant [8]. In general, this is a far smaller rotation frequency (either of the plasma or the shell) than that needed to stabilize the resistive shell mode in the presence of a single shell.

2.5 The "Chicken Wire" Shell

As a simple example, suppose that the network of inductors and resistors discussed in previous sections is, in fact, a network of uniform wires of diameter d. The poloidal and toroidal resistances are

$$R_\theta = \frac{4 r_w \Delta\theta}{\sigma_w \pi d^2}, \tag{43}(a)$$

$$R_\phi = \frac{4 R_0 \Delta\phi}{\sigma_w \pi d^2}, \tag{43}(b)$$

respectively, where σ_w is the conductivity of the wire. It follows from Eq. (16) that

$$\tau_w \simeq \frac{\pi}{4}\frac{\mu_0 \sigma_w d^2}{\Delta\theta} = \mu_0 \sigma_w r_w \delta_w, \tag{44}$$

where

$$\delta_w \simeq \frac{\pi d^2}{4 r_w \Delta\theta} \tag{45}$$

is the thickness of the uniform shell which contains the same volume of metal as the wires. Here, it is assumed that

$$n^2 r_w \Delta\phi \ll m^2 R_0 \Delta\theta. \tag{46}$$

According to Eq. (44), the time constant of the network is approximately the same as that which would be obtained by melting down the wires and recasting them as a uniform shell (with the same minor radius as the network).

The poloidal and toroidal inductances are (see Appendices A and B)

$$L_\theta \sim r_w \Delta\theta \, \frac{\mu_0}{2\pi} \left(\frac{\pi r_w}{m R_0 \Delta\phi} + \ln\left(\frac{R_0 \Delta\phi}{d} \right) \right), \tag{47}(a)$$

$$L_\phi \simeq R_0 \Delta\phi \, \frac{\mu_0}{2\pi} \left(\frac{\pi}{m \Delta\theta} + \ln\left(\frac{r_w \Delta\theta}{d\,\pi} \right) + O(m\Delta\theta) \right), \tag{47}(b)$$

respectively. Thus, according to Eq. (17)

$$\Delta_c \simeq \frac{2\pi}{\Delta\theta \ln(r_w \Delta\theta / d\,\pi)}. \tag{48}$$

Note that $O(n r_w / m R_0)$ is negligible (by definition) in the large aspect ratio, low β tokamak limit. Equation (48) implies that if the network is fine (i.e. $\Delta\theta \ll 2\pi$) then it is difficult for an external kink mode to escape between the wires (i.e. $\Delta_c \gg 1$). However, if the wires are very thin (i.e. $d \ll r_w$) then it becomes easier for the mode to escape (i.e. Δ_c is reduced).

2.6 Summary

In Section 2.2 it is demonstrated that if a tokamak plasma is surrounded by a network of resistors and inductors then the network acts like an incomplete resistive shell as far as its effect on external kink modes is concerned. Section 2.3 shows that a simple feedback scheme applied to such a network causes it to act like a fake *rotating* shell. It is demonstrated in Section 2.4 that the combination of a stationary shell and a fake rotating shell is able to completely stabilize the resistive shell mode. Some important parameters are calculated in Section 2.5 for the specific case of a network made up of uniform cylindrical wires.

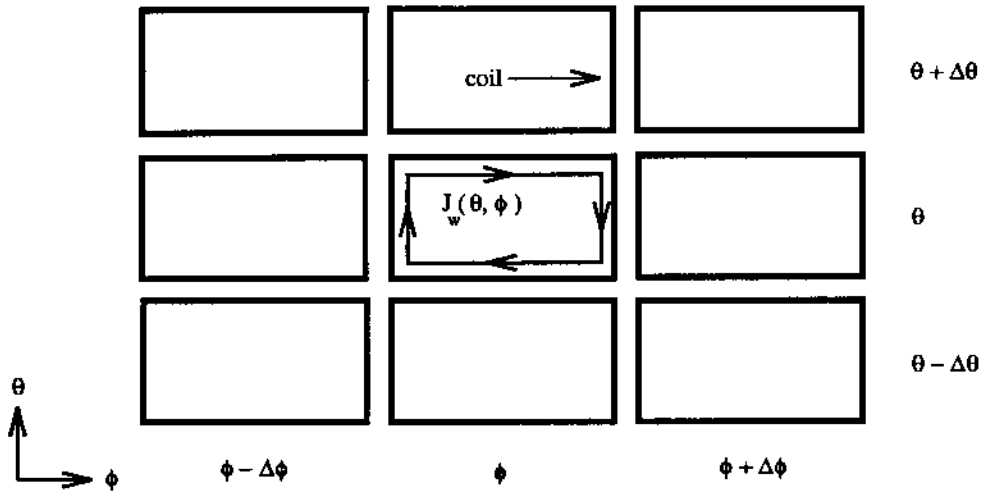

Figure 3: *Schematic diagram showing part of the intelligent shell, which is a two dimensional array of close fitting coils surrounding the plasma. A current $J_w(\theta, \phi)$ circulates around the loop centred on (θ, ϕ).*

3 The Intelligent Shell

3.1 Introduction

It is instructive to compare the stabilization scheme for the resistive shell mode which is outlined in Section 2 to the most promising scheme currently in the literature; namely, the "intelligent shell" [5].

3.2 Preliminary Analysis

Consider a shell made up of a two dimensional array of close fitting coils (see Fig. 3). Let $\Delta\theta$ and $\Delta\phi$ be the angular spacings of the centres of the coils in the poloidal and toroidal directions, respectively.

Suppose that a current $J_w(\theta, \phi)$ flows around the coil, or loop, centred on (θ, ϕ). The currents flowing in the array are approximated as a smoothed out distribution with radially integrated current density $\delta\mathbf{I}_w(\theta, \phi)$. It is easily demonstrated that $\delta\mathbf{I}_w \simeq \nabla J_w \wedge \hat{\mathbf{r}}$ (see Eq. (3)).

The circuit equation for the loop centred on $(\theta,\, \phi)$ is

$$-\gamma\, \delta B_{r\,\mathrm{plasma}}\, \Delta A - \gamma L J_w = R J_w, \tag{49}$$

where $\Delta A = r_w R_0 \Delta\theta \Delta\phi$ is the area of the loop, L is its inductance, and R is its resistance. Equations (6) and (12) yield

$$\mathrm{i}\, \gamma m R_0 \Delta\theta \Delta\phi \left(1 + \frac{\Delta_w}{2m}\right) \hat{\Psi}_w = -(R + \gamma L) \hat{J}_w, \tag{50}$$

which can be combined with Eq. (9) to give

$$\gamma \tau_w = \frac{\Delta_w}{1 - \Delta_w/\Delta_c}, \tag{51}$$

where

$$\tau_w = \frac{\mu_0 m^2 R_0 \Delta\theta \Delta\phi}{R}, \tag{52}$$

and

$$\Delta_c = \frac{\mu_0 m^2 R_0 \Delta\theta \Delta\phi}{\tilde{L}}. \tag{53}$$

Here,

$$\tilde{L} = L - \frac{\mu_0 m^2 R_0 \Delta\theta \Delta\phi}{2m}. \tag{54}$$

Note that Eq. (51) has the same form as the dispersion relation for an incomplete resistive shell of time constant τ_w located at radius r_w [6]. The m/n external kink mode is ideally unstable whenever $\Delta_w \geq \Delta_c$. The ideal mode escapes through the centres of the loops, so it is not shielded from the region $r > r_w$, as would be the case for a conventional shell.

3.3 Feedback

Suppose that each loop in the array (these are termed power loops) is accompanied by a loop of equal area connected to a high impedance voltage sensor which measures the local rate of change of the magnetic flux escaping through the array (see Fig. 4). Suppose, further, that the signal detected by the sensor loop is amplified by a factor G and fed into the associated

power loop. The voltage detected by the sensor loop centred on $(\theta,\,\phi)$ is $\widehat{V}\exp[\mathrm{i}\,(m\theta-n\phi)]$, where

$$\widehat{V}\simeq-\gamma\left(\mathrm{i}\,mR_0\Delta\theta\Delta\phi\left(1+\frac{\Delta_w}{2m}\right)\widehat{\Psi}_w+L\widehat{J}_w\right). \tag{55}$$

The modified circuit equation for the power loop centred on $(\theta,\,\phi)$ is

$$(1+G)\widehat{V}=R\widehat{J}_w, \tag{56}$$

which gives the dispersion relation

$$\gamma\widehat{\tau}_w=\frac{\Delta_w}{1-\Delta_w/\Delta_c}, \tag{57}$$

where

$$\widehat{\tau}_w=(1+G)\tau_w. \tag{58}$$

Thus, the feedback increases the effective time constant of the shell by a factor $1+G$. Clearly, if the gain G is made sufficiently large then it is possible to make the effective time constant longer than the pulse length of the tokamak discharge. In this case, the shell acts, to all intents and purposes, like an ideal conductor and is, therefore, able to completely stabilize the external kink mode. Note, however, that stabilization is only possible if the array of coils is located sufficiently close to the plasma to convert the ideal external kink mode into a resistive shell mode; i.e. if $\Delta_w<\Delta_c$.

3.4 Example

Suppose that the intelligent shell is made up of closely interlocking cylindrical conductors (see Fig. 5). Let d be the radius of the outer conductor and $d-c$ the radius of the inner conductor, where $c/d\ll 1$. Suppose that both conductors possess the same cross sectional area, $\delta A/2$. Consider, for the sake of simplicity, the limit in which the poloidal inductance and resistance of the network are negligible. This limit corresponds to $r_w\Delta\theta\ll R_0\Delta\phi$ if the inductance and resistance per unit length are the same in the poloidal and toroidal directions.

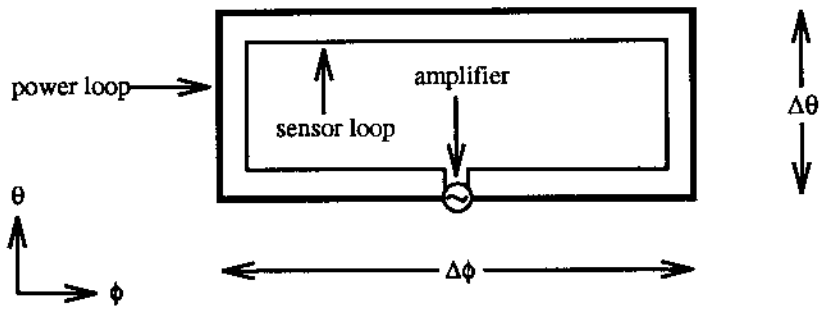

Figure 4: *Schematic diagram showing the feedback scheme for a single element of the intelligent shell. The signal detected by the high impedance sensor loop is amplified and then fed into the low impedance power loop.*

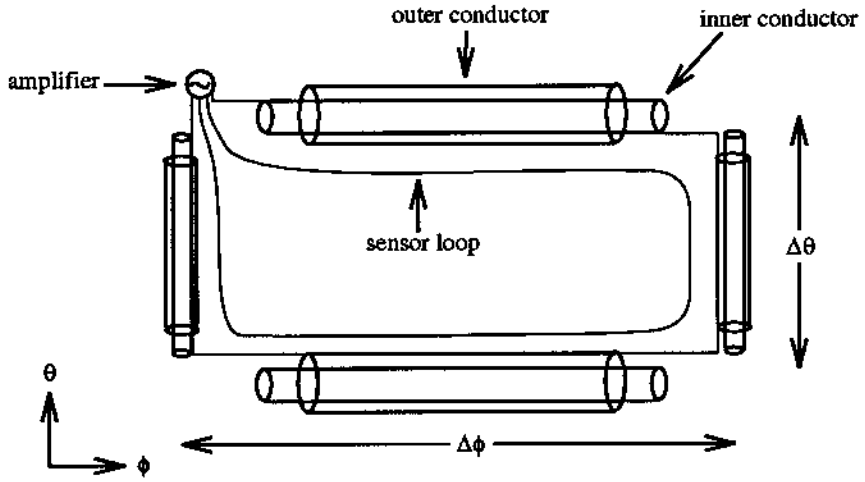

Figure 5: *Schematic diagram showing a single coil in a particular implementation of the intelligent shell in which the coils consist of interlocking cylindrical conductors (e.g. co-axial cables). Those conductors which are shown unconnected in the diagram, in fact, form parts of the circuits of the surrounding coils. Every coil in the array is connected up in an analogous manner.*

The resistance of a loop is given by

$$R \simeq \frac{4R_0\Delta\phi}{\sigma_w \delta A}, \tag{59}$$

where σ_w is the conductivity of the conductors. It follows from Eq. (52) that

$$\tau_w \simeq \frac{(m\Delta\theta)^2}{4}\,\mu_0\sigma_w r_w \delta_w, \tag{60}$$

where

$$\delta_w = \frac{\delta A}{r_w \Delta\theta} \tag{61}$$

is the thickness of the uniform shell which contains the same volume of metal as the conductors. Clearly, the time constant of the array is significantly less than that which would be obtained by melting down the conductors and recasting them as a uniform shell (with the same minor radius as the array).

The inductance of a loop is given by

$$L \simeq R_0\Delta\phi\frac{\mu_0}{2\pi}\frac{c}{d} + (m\Delta\theta)^2 R_0\Delta\phi\frac{\mu_0}{2\pi}\left(\frac{\pi}{m\Delta\theta} + \ln\left(\frac{r_w\Delta\theta}{d\,\pi}\right)\right), \tag{62}$$

where use has been made of Appendix B. The first term on the right-hand side of the above expression comes from magnetic fields trapped in the regions between the inner and outer conductors. The second term comes from fields which leak outside the conductors. According to Eq. (53),

$$\Delta_c = \frac{2\pi}{\Delta\theta\ln(r_w\Delta\theta/d\,\pi)}\frac{(m\Delta\theta)^2\ln(r_w\Delta\theta/d\,\pi)}{c/d + (m\Delta\theta)^2\ln(r_w\Delta\theta/d\,\pi)}. \tag{63}$$

It can be seen, by comparison with Eq. (48), that the fields trapped between the inner and outer conductors significantly increase the inductance of an array of independent coils compared to that of a similar network. The net result is that it is easier for an ideal mode to escape through an array of unconnected conductors than through a network of interconnected conductors of similar dimensions (i.e. Δ_c is smaller in the former case). Note that if the array is fine (i.e. $m\Delta\theta \ll 1$) then it is particularly easy for an ideal mode to

escape into the region $r > r_w$. However, if the inner and outer conductors are extremely closely spaced (i.e. $c/d \to 0$) then the inductance of the array approaches that of a similar network.

3.5 Summary

In Section 3.2 it is demonstrated that if a tokamak plasma is surrounded by an array of unconnected coils then the array acts like an incomplete resistive shell as far as its effect on external kink modes is concerned. Section 3.3 shows that a simple feedback scheme applied to such an array causes its effective time constant to increase. According to Section 3.4, the intrinsic time constant of an array of coils is very much smaller than that of a similar network. Moreover, the inductance of an array is much larger than that of a similar network. Consequently, it is much easier for an ideal mode to escape through an array of unconnected coils than through a network of interconnected conductors.

4 Practical Considerations

4.1 Introduction

In any feedback scheme the four most important parameters are the gain G of the amplifiers, the bandwidth Δf of the signals to which they must respond, the current I which they need to supply, and the power P which they must put out. In this section these parameters are estimated for both the fake rotating shell and intelligent shell concepts.

4.2 The Fake Rotating Shell

The gain, G, is defined as the ratio of the voltage generated in a sensor loop to that which is put out into the network by the associated amplifier. It is easily seen from Section 2.3 that

$$G = \frac{1}{|\gamma \tau|}. \tag{64}$$

It follows from Section 2.4 that the critical gain needed to achieve stabilization of the resistive shell mode is

$$G_c = \frac{\tau_1}{m\Delta\theta\,\tau_2}\left(\frac{E_2}{E_{12}}\right)^2\left(\frac{1/E_{2\infty}-1/E_2}{1/E_{2\infty}-1/E_{2c}}\right), \tag{65}$$

where

$$m\Delta\theta\,\tau_2 = \frac{\mu_0 m}{r_\phi}. \tag{66}$$

Here, r_ϕ is the resistance per unit length of the toroidal legs of the network. Recall that τ_1 is the time constant of the stationary shell, τ_2 is the effective time constant of the fake shell produced by the network, $E_{2\infty}$ is the shell stability index for the fake shell calculated in the absence of the stationary shell, and E_{2c} is the critical value of $E_{2\infty}$ above which the ideal external kink mode becomes unstable. It follows from Eqs. (37)–(39) that

$$G_c = \frac{\tau_1}{m\Delta\theta\,\tau_2}\frac{(1+E_{2\infty}/2m)(r_2/r_1)^{2m}-E_{2\infty}/2m}{1-E_{2\infty}/E_{2c}} \tag{67}$$

Here, r_1 is the radius of the stationary shell and r_2 is the radius of the network. It is assumed that $\tau_1 \gg \tau_2$ in Section 2.4 so it follows from Eq. (67) that $G_c \gg 1/m\Delta\theta$. It also follows that the *optimum* position for the network is that it should be placed as close as possible to the plasma. Note, however, that if

$$r_2 < r_1\left(\frac{E_{2\infty}/2m}{1+E_{2\infty}/2m}\right)^{1/2m} \tag{68}$$

then a mode which co-rotates with the fake shell but does not penetrate the stationary shell, and grows on the relatively fast timescale τ_2, becomes unstable (see Section 2.4). The most *sensible* position for the network is just outside the stationary shell. In this configuration the critical gain is relatively small, i.e.

$$G_c = \frac{\tau_1}{m\Delta\theta\,\tau_2}\frac{1}{1-E_{2\infty}/E_{2c}}, \tag{69}$$

and the stationary shell shields the network sensor loops from any extraneous high frequency signals generated by the plasma. Thus, the bandwidth of the signals detected by the feedback

amplifiers is

$$\Delta f \sim \frac{1}{\tau_1}. \tag{70}$$

It is easily demonstrated that

$$\tilde{r} = r_2 \left(1 + \frac{2m}{E_{2\infty}}\right)^{1/2m}, \tag{71}$$

where $\tilde{r}$ is the critical radius of a perfectly conducting shell surrounding the plasma for which the m/n free boundary ideal external kink mode is marginally stable. It is sometimes convenient to use $\tilde{r}$, instead of $E_{2\infty}$, to parameterize the stability of the plasma. Equation (69) can be written

$$G_c = \frac{\tau_1}{m\Delta\theta\,\tau_2}\frac{(\bar{r})^{2m} - (r_2)^{2m}}{(\bar{r})^{2m} - (\hat{r}_2)^{2m}}, \tag{72}$$

where

$$\hat{r}_2 = r_2 \left(1 + \frac{2m}{E_{2c}}\right)^{1/2m} \tag{73}$$

is the effective radius of the fake shell (see Eq. (20)).

The voltage put out by a particular amplifier is $V \sim b_r \Delta A/\tau$, where b_r is the local radial magnetic field and ΔA is the area of a network loop. The current put out by the amplifier is given by $I \sim V/R_\phi$. It follows that

$$I \sim \frac{r_2\, b_r}{\mu_0}\frac{m\Delta\theta}{m^2}, \tag{74}$$

where use has been made of Eq. (29)(a) and $\Omega_2\tau_2 \sim O(1)$. The power put out by the amplifier is $P \sim VI$, yielding

$$P \sim \frac{r_2\,(b_r)^2}{\mu_0}\frac{\Delta A}{m^2\tau_2}. \tag{75}$$

Consider a specific example. Suppose that the minor and major radii of the plasma are $a = 1$ m and $R_0 = 3$ m, respectively. Suppose that the $m = 2/n = 1$ free boundary external kink mode is unstable. Suppose that the stationary shell and the network are both located 1.1 minor radii from the centre of the plasma (i.e. $r_1 = r_2 = 1.1\,a$). Suppose that there are

20 network loops in the poloidal direction and 10 in the toroidal direction; i.e. $\Delta\theta = 2\pi/20$ and $\Delta\phi = 2\pi/10$. Suppose that the stationary shell is made of 5 mm thick stainless steel of resistivity $7.2\times10^{-7}\ \Omega\,\mathrm{m}$ [10]. Finally, suppose that the network is made of 2.5 mm diameter copper wires of resistivity $1.7\times10^{-8}\ \Omega\,\mathrm{m}$ [11].

The time constant of the stationary shell is $\tau_1 = 9.6\,\mathrm{ms}$. The effective time constant of the fake shell is $\tau_2 = 1.2\,\mathrm{ms}$ (see Eq. (44)). The critical shell stability index for the fake shell is $E_{2c} = 6.5$ (see Eq. (48)). This implies that the fake shell acts like a conventional shell whose effective radius is $\hat{r}_2 = 1.24\,a$ (see Eq. (73)). The critical gain needed to stabilize the resistive shell mode is (see Eq. (72))

$$G_c \sim 13\,\frac{(\tilde{r}/1.24)^4 - 0.62}{(\tilde{r}/1.24)^4 - 1}, \tag{76}$$

where $\tilde{r}$ is measured in meters. The bandwidth of the signal detected by each amplifier is $\Delta f \sim 100\,\mathrm{Hz}$. The current which each amplifier needs to provide is $I \sim 14\,b_r$ A (see Eq. (74)), where b_r is measured in gauss. Finally, the power drawn from each amplifier is $P \sim 1.2\,(b_r)^2\,\mathrm{W}$ (see Eq. (75)).

It can be seen that the gain, bandwidth, and power requirements of the fake rotating shell concept are extremely modest. The current requirement is more onerous (for instance, each amplifier must supply over 100 amperes in order to stabilize a modest 10 gauss perturbation) and is likely to be the limiting factor for this scheme.

4.3 The Intelligent Shell

For the intelligent shell concept the gain needed to stabilize the resistive shell mode is $G \sim \tau_p/\tau_w$, where τ_w is the effective time constant of the shell and τ_p is the pulse length of the discharge. The bandwidth of the signals detected by the feedback amplifiers can, in principle, be quite large unless the intelligent shell is shielded from the plasma by a conventional shell (i.e. the vacuum vessel). Assuming that the mode grows on the slowed

down time constant of the shell (i.e. $\gamma G \tau_w \sim 1$), the current which each amplifier needs to supply is

$$I \sim \frac{r_w b_r}{\mu_0} \frac{1}{m^2}. \tag{77}$$

The power drawn by each amplifier is

$$P \sim \frac{r_w (b_r)^2}{\mu_0} \frac{\Delta A}{m^2 \tau_w}. \tag{78}$$

Consider a specific example. Suppose that all of the parameters are the same as in the previous section, except that there is no stationary shell (or, equivalently, the time constant of the stationary shell is much less than the effective time constant of the intelligent shell), and the network is replaced by an array of interlocking copper conductors whose total cross sectional area is the same as that of a 2.5 mm wire. Suppose that the outer radius of the conductors is 5 mm and that the ratio of the spacing of the inner and outer conductors to the radius of the outer conductors is 0.2 (i.e. $c/d = 0.2$). Suppose, finally, that the pulse length of the discharge is 10 seconds.

The effective time constant of the intelligent shell is $\tau_w = 0.11$ ms (see Eq. (60)). The critical shell stability index for the array is $\Delta_c = 5.6$ (see Eq. (63)). This implies that the array acts like a conventional shell whose effective radius is $1.26\,a$. The amplifier gain required to stabilize the resistive shell mode is $G \sim 9 \times 10^4$. The bandwidth of the signal detected by each amplifier is similar to that for the fake rotating shell provided that the intelligent shell lies outside the vacuum vessel. The current which each amplifier needs to supply is $I \sim 22\,b_r$ A. Finally, the power drawn from each amplifier is $P \sim 13\,(b_r)^2$W.

It can be seen that the current, bandwidth, and power requirements of the intelligent shell are similar to those of the fake rotating shell. However, the intelligent shell concept requires a large amplifier gain. This is likely to lead to control engineering problem (large gain amplifiers are prone to instabilities) and is certainly the limiting factor for this scheme.

4.4 Summary

The gain, bandwidth, current, and power requirements of the fake rotating shell concept lie well within the range of cheap, reliable, and readily available amplifiers. The intelligent shell concept only works with expensive (and unreliable) high gain amplifiers.

5 Summary and Conclusions

In Section 2 it is demonstrated that a network of conductors surrounding a tokamak plasma acts very much like an incomplete resistive shell as far as its effect on the free boundary external kink mode is concerned. It is further shown that a simple feedback scheme applied to such a network causes it to act like a rotating resistive shell. As is well known [8], the combination of a stationary and a rotating shell can very easily stabilize the resistive wall mode. In Section 3 it is demonstrated that an array of independent coils surrounding a tokamak plasma also acts like an incomplete resistive shell. A simple feedback scheme applied to such an array causes its effective L/R time to increase [5]. In principle, the L/R time could be made longer than the pulse length of the plasma, but this requires extremely high gain feedback. It is shown that a network of interconnected conductors has a significantly longer L/R time than a similar array of unconnected coils. Furthermore, a network is better able to contain an external kink mode than an array. In Section 4 it is demonstrated that the fake rotating shell stabilization scheme outlined in Section 2 can be implemented with low gain, low bandwidth, low current, low power amplifiers.

The feedback gain needed to stabilize the resistive wall mode in the fake rotating shell concept is so low (see Section 4.2) that the required amplification of the signals detected by the feedback circuits could, in principle, be achieved by using multi-turn sensor loops. In other words, the sensor loops shown in Fig. 2 could consist of twenty (say) turns of wire, instead of a single turn (as shown in the figure). This would automatically amplify the

detected signal by a factor twenty, which would probably be sufficient for stabilization of the resistive shell mode. The signal could then be integrated and then fed into the main network. The primary constraint on the fake rotating shell concept is the fact that the signals detected by the feedback circuits have to be accurately integrated over a long time period (i.e. the pulse length of the discharge). If the integrated signals become inaccurate after some time T, say, then one would expect the resistive shell mode to reappear as a mode growing through both the real and the fake shells on about the timescale T. The need for integration could be completely avoided by using Hall probes rather than sensor loops for signal detection in the feedback circuits.

There is an interesting difference in the basic stabilization strategy employed by the intelligent shell and the fake rotating shell concepts. In the former scheme, the feedback circuits detect magnetic flux leaking through the vacuum vessel and attempt to push it back through the vessel (i.e. radially inwards). In the latter scheme, the feedback circuits detect flux leaking through the vacuum vessel and attempt to push it *sideways* (i.e. in the poloidal direction). This has the effect of causing the mode leaking through the vessel to rotate. The mode is then suppressed by eddy currents excited in the vacuum vessel. Thus, in the fake rotating shell concept most of the work is done by the vacuum vessel. This is in marked contrast to the intelligent shell concept, where all of the work is done by the feedback circuits. Hence, the low gain required by the former concept, and the very high gain required by the latter.

It is important to check that the feedback controlled network described in Section 2, which is central to the fake rotating shell concept, is intrinsically stable. This is done in Appendix C. It is demonstrated that if the fake rotating shell scheme is expected to stabilize resistive shell modes whose maximum poloidal and toroidal mode numbers are m and n, respectively, then the *minimum* number of network cells in the poloidal and toroidal directions required to achieve this is $2m + 1$ and $2n + 1$, respectively. Thus, in principle,

it is possible to stabilize the 1/1, 2/1, and 3/1 modes simultaneously by using a network consisting of four cells in the toroidal direction and eight in the poloidal direction. That is, a total of thirty two interlinked feedback controlled circuits.

In conclusion, the fake rotating shell concept appears quite capable of stabilizing the resistive shell mode in a long pulse tokamak discharge at relatively low cost using existing technology. This scheme is more reactor relevant than the alternative approach of forcing the plasma to rotate rapidly.

Acknowledgments

One of the authors (R.F.) is indebted to General Atomics of La Jolla, CA, for the hospitality shown during his visit in the Summer of 1995.

This research was funded by the U.S. Department of Energy under contracts DE-FG05-80ET-53088 and DE-AC03-89ER-51114.

Appendices

A Estimation of L_θ

Consider the network of wires described in Section 2.5. The current flowing in poloidally directed wires is approximately constant over a poloidal wavelength, $\pi r_w/m$. Thus, a poloidally directed wire can be approximated as a wire carrying a uniform current provided that the perpendicular distance from the wire is much less than the poloidal wavelength. This approximation breaks down at the Nth wire distant from the wire in question, where

$$N = \frac{\pi r_w}{m R_0 \Delta\phi} \gg 1. \tag{A.1}$$

Assuming a uniform phase variation of the poloidal current from wire to wire (since the poloidal wavelength is much less than the toroidal wavelength) the currents flowing in each wire are as indicated in Fig. 6. Thus, the poloidal inductance of a given network loop can be crudely approximated as

$$L_\theta \sim r_w \Delta\theta \frac{\mu_0}{2\pi}\left[\ln\left(\frac{2R_0\Delta\phi}{d}\right) + 2\ln\frac{2}{1} + 3\ln\frac{3}{2}\cdots + N\ln\frac{N}{N-1}\right], \tag{A.2}$$

which reduces to

$$L_\theta \sim r_w \Delta\theta \frac{\mu_0}{2\pi}\left(\frac{\pi r_w}{m R_0 \Delta\phi} + \ln\left(\frac{R_0\Delta\phi}{d}\right) + O(\ln N)\right). \tag{A.3}$$

In Eq. (A.2) the contributions from wires whose perpendicular distances from the loop in question exceed the poloidal wavelength are assumed to be negligible. A more exact calculation of the poloidal inductance using the Biot-Savart law yields essentially the same result that given above.

B Evaluation of L_ϕ

Consider the network of wires described in Section 2.5. In a large aspect ratio tokamak the toroidal wavelength of the m/n mode is much greater than its poloidal wavelength, so any

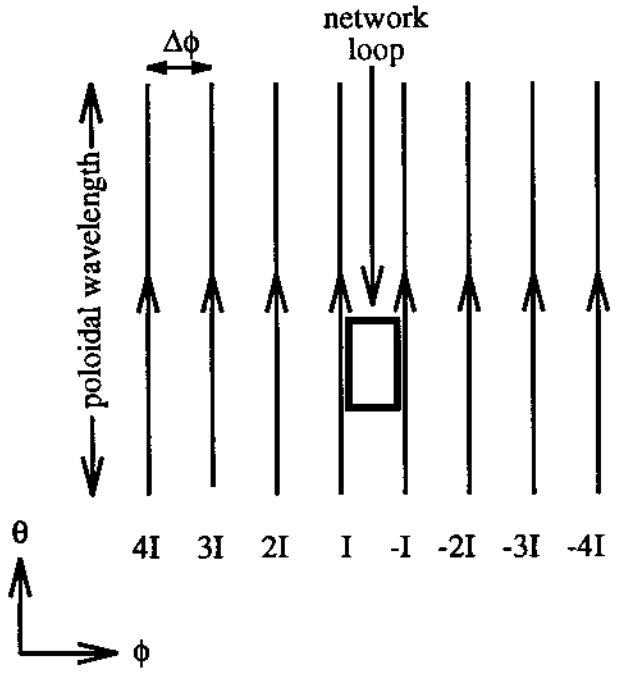

Figure 6: *Schematic diagram showing the array of poloidal currents used to estimate L_θ. Here, I, $2I$, etc. denote the currents flowing in each wire.*

phase variation of the network currents in the toroidal direction can be ignored. In fact, the system can be treated as a set of infinite toroidal wires each carrying a uniform current whose phase varies slowly from wire to wire in the poloidal direction (see Fig. 7).

The toroidal inductance term in Eq. (4) actually represents

$$V = -\gamma R_0 \Delta\phi \frac{\mu_0}{2\pi}\left[I(\theta)\ln\left(\frac{2r_w\Delta\theta}{d}\right) - I(\theta-\Delta\theta)\ln\left(\frac{2r_w\Delta\theta}{d}\right)\right.$$

$$+I(\theta+\Delta\theta)\ln\frac{2}{1} - I(\theta-2\Delta\theta)\ln\frac{2}{1}$$

$$\left.+I(\theta+2\Delta\theta)\ln\frac{3}{2} - I(\theta-3\Delta\theta)\ln\frac{3}{2} + \ldots\right], \tag{B.1}$$

where

$$I(\theta+j\Delta\theta) = J_w(\theta+j\Delta\theta) - J_w(\theta+(j+1)\Delta\theta)$$

$$\simeq -\Delta\theta\,\frac{\partial J_w(\theta+(j+1/2)\Delta\theta)}{\partial\theta}. \tag{B.2}$$

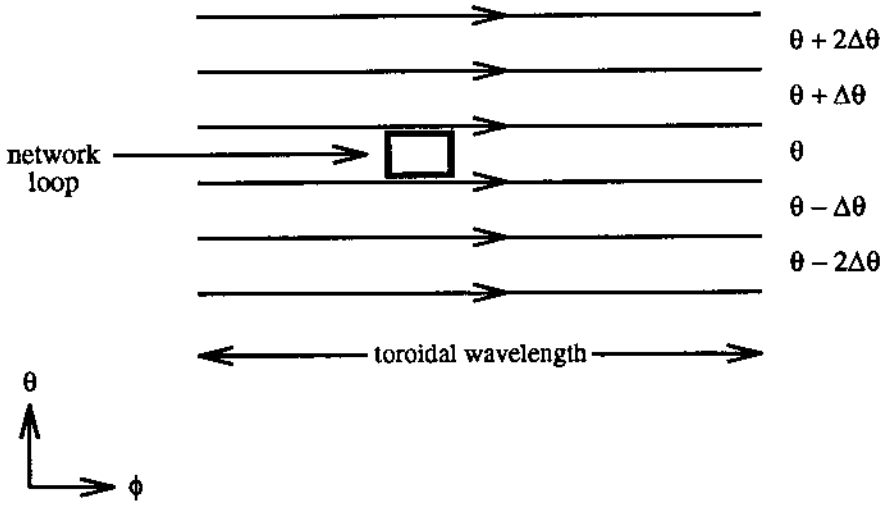

Figure 7: *Schematic diagram showing the array of toroidal currents used to evaluate* L_ϕ.

Thus,

$$V = -\gamma R_0 \Delta\theta \, \frac{\mu_0}{2\pi} \, 2m\Delta\theta \, \hat{J}_w \exp(\mathrm{i}\, m\theta) \left[\sin(m\Delta\theta/2) \ln\left(\frac{2r_w\Delta\theta}{d}\right) \right.$$

$$\left. + \sin(3m\Delta\theta/2) \ln\frac{2}{1} + \sin(5m\Delta\theta/2) \ln\frac{3}{2} + \cdots \right], \tag{B.3}$$

where use has been made of Eq. (6)(c). Now

$$V = -\gamma \, (m\Delta\theta)^2 \hat{J}_w \exp(\mathrm{i}\, m\theta) \, L_\phi, \tag{B.4}$$

so

$$L_\phi = R_0 \Delta\phi \, \frac{\mu_0}{2\pi} \frac{1}{\alpha} \left(\sin\alpha \, \ln\left(\frac{2r_w\Delta\theta}{d}\right) + \mathcal{I} \right), \tag{B.5}$$

where

$$\alpha = \frac{m\Delta\theta}{2} \ll 1, \tag{B.6}$$

and

$$\mathcal{I} = \sum_{n=1}^{\infty} \sin(\,(2n+1)\alpha\,) \ln\left(1 + \frac{1}{n}\right). \tag{B.7}$$

It is easily demonstrated that

$$\mathcal{I} = \frac{\pi}{2} - \alpha \ln 2\pi + O(\alpha^2). \tag{B.8}$$

Thus,

$$L_\phi = R_0 \Delta\phi \frac{\mu_0}{2\pi} \left(\frac{\pi}{m\Delta\theta} + \ln\left(\frac{r_w \Delta\theta}{d\,\pi} \right) + O(m\Delta\theta) \right). \tag{B.9}$$

Note that this calculation neglects the curvature of the network, so the result is only accurate for $m \gg 1$.

C Network Stability

It is important to verify that the feedback controlled network discussed in Section 2 is intrinsically stable. Consider, for the sake of simplicity, the limit $n^2 r_w \Delta\phi \ll m^2 R_0 \Delta\phi$ in which the poloidal inductance and resistance of the network are negligible. In the absence of plasma (i.e. $\delta B_{r\,\mathrm{plasma}} = 0$) the circuit equation (4) for the network without any feedback yields

$$\gamma = -\frac{R_\phi}{L_\phi}. \tag{C.1}$$

A slight generalization of the analysis used in Appendix B, in order to deal with modes of arbitrary poloidal wavelength, yields

$$L_\phi(\alpha) = R_0 \Delta\phi \frac{\mu_0}{2\pi} \left[\ln\left(\frac{2 r_w \Delta\theta}{d} \right) + J(\alpha) \right], \tag{C.2}$$

where

$$\alpha = \frac{m\Delta\theta}{2}, \tag{C.3}$$

and

$$J(\alpha) = \sum_{n=1}^{\infty} \frac{\sin(\,(2n+1)\alpha\,)}{\sin\alpha} \ln\left(1 + \frac{1}{n}\right). \tag{C.4}$$

Note that

$$J(\alpha + k\pi) = J(\alpha), \tag{C.5)(a}$$

$$J(\pi - \alpha) = J(\alpha), \tag{C.5)(b}$$

where k is an integer. It is easily demonstrated that $J(\alpha)$ is a monotonically decreasing function of α in the range $0 < \alpha < \pi/2$. For $\alpha \ll 1$,

$$J(\alpha) \simeq \frac{\pi}{2\alpha} - \ln(2\pi) + O(\alpha). \tag{C.6}$$

The minimum value of $J(\alpha)$ occurs when $\alpha = \pi/2$; in fact,

$$J(\pi/2) = -\ln(\pi/2). \tag{C.7}$$

Note that $L_\phi(\pi/2) > 0$, since $r_w \Delta\theta > d$ (i.e. the poloidal spacing between the wires always exceeds their diameter) and $\ln 2 > \ln(\pi/2)$. Thus,

$$L(\alpha) \geq 0 \tag{C.8}$$

for all α. This demonstrates (from Eq. (C.1)) that the network is never unstable in the absence of feedback. The network is marginally stable to modes whose poloidal wavelength divided by an integer equals the poloidal wavelength of the network. Such modes excite no eddy currents in the network, by symmetry, hence their energy cannot be dissipated by joule heating in the wires making up the network (this is the usual mechanism by which modes are damped).

According to Section 2.3, the feedback controlled network satisfies the circuit equation

$$\gamma + \frac{(1 + \exp(\mathrm{i}\, m\Delta\theta))}{\tau} = -\frac{R_\phi}{L_\phi}, \tag{C.9}$$

which reduces to the dispersion relation

$$\gamma(\alpha) = -\frac{R_\phi}{L_\phi(\alpha)} - 2\,\frac{(\sin\alpha)^2}{\tau} + \mathrm{i}\,\frac{\sin 2\alpha}{\tau}. \tag{C.10}$$

Note that

$$\gamma(\alpha + k\pi) = \gamma(\alpha), \tag{C.11}$$

where k is an integer. According to Eq. (C.10), the feedback controlled network is never unstable, but is marginally stable to modes whose poloidal wavelength divided by an integer

equals the poloidal wavelength of the network. Such modes satisfy

$$\alpha = k\pi, \tag{C.12}$$

where k is an integer. Feedback gives rise to enhanced damping of modes for which $\alpha \neq k\pi$. The feedback also causes the modes to propagate; i.e. it causes the network to act like it is rotating. However, the network appears non rotating to all modes whose poloidal wavelength divided by an integer equals *twice* the poloidal wavelength of the network. Such modes satisfy

$$\alpha = k\frac{\pi}{2}, \tag{C.13}$$

where k is an integer.

According to the main text, the network is only capable of stabilizing a given resistive shell mode if it appears to possess a *positive* (i.e. non zero) inductance and a *non zero* effective rotation velocity to a mode with that poloidal wavelength. This is guaranteed to be the case if

$$\alpha < \frac{\pi}{2}. \tag{C.14}$$

Suppose that the network is required to suppress all resistive shell modes whose poloidal wavenumbers lie in the range 1 through m. According to Eq. (C.14), the *minimum* number of network cells in the poloidal direction needed to achieve this is

$$M = 2m + 1. \tag{C.15}$$

Here, $\Delta\theta = 2\pi/M$. Likewise, if the network is required to stabilize all resistive shell modes whose toroidal mode numbers lie in the range 1 through N, then the *minimum* number of network cells in the toroidal direction needed to achieve this is

$$N = 2n + 1. \tag{C.16}$$

Here, $\Delta\phi = 2\pi/N$. It is advantageous to have $M > 2m + 1$ since this reduces the L/R time of the network and, therefore, brings down the feedback gain required for stabilization of the resistive shell mode. Likewise, it is advantageous to have $N > 2n + 1$.

References

[1] F. Troyon, R. Gruber, H. Saurenmann, S. Semenzato, and S. Succi, Plasma Phys. Contrld. Nucl. Fusion **26**, 209 (1984).

[2] J.A. Wesson, Nucl. Fusion **18**, 87 (1978).

[3] D. Pfirsch, and H. Tasso, Nucl. Fusion **11**, 259 (1971).

[4] A. Bondeson, and D.J. Ward, Phys. Rev. Lett. **72**, 2709 (1994).

[5] C.M. Bishop, Plasma Phys. Contrld. Nucl. Fusion **31**, 1179 (1989).

[6] R. Fitzpatrick, Phys. Plasmas **1**, 2931 (1994).

[7] R. Fitzpatrick, and A.Y. Aydemir, *Stabilization of the resistive shell mode in tokamaks*, to appear in Nuclear Fusion.

[8] C.G. Gimblett, Plasma Phys. Contrld. Nucl. Fusion **31**, 2183 (1989).

[9] R. Fitzpatrick, R.J. Hastie, T.J. Martin, and C.M. Roach, Nucl. Fusion **33**, 1533 (1993).

[10] E.A. Solano, private communication. This figure is for SS304.

[11] *Handbook of chemistry and physics*, Edited by D.R. Lide, (Chemical Rubber Company Press, Baca Raton, Florida, 1995).